Partial Rhombencephalosynapsis and Chiari Type II Malformation in a Child: a True Association Supported by DTI Tractography

Laura Merlini · Joel Fluss · Christian Korff · Sylviane Hanquinet

Abstract Partial rhombencephalosynapsis (PRECS) has been recently reported in association with Chiari II (CII). However, its existence as a true malformation is challenged due to the anatomical changes potentially induced by CII. The aim of this report was to investigate the contribution of midbrain/hindbrain tractography in this setting. A 13-year-old boy with a known CII malformation and operated myelomeningocele was referred for brain imaging after a first complex partial seizure. In addition to the classical features of CII, MRI showed partially fused cerebellar hemispheres and multiple supratentorial abnormalities. Diffusion tensor imaging (DTI) color map and tractography showed absent transverse fibers on the midsection of the cerebellum, scarce fibers of the middle cerebellar peduncle (MCP), absence of the middle pontine crossing tract, and fibers running vertically in the medial part of the cerebellum. Vertical mediocerebellar fibers are a feature of classical RECS and the paucity or absence of MCP fibers is mainly described in CII. In our patient, DTI and FT therefore demonstrated structural characteristics of both RECS and CII confirming their potential coexistence and suggesting possible shared embryological pathway.

Keywords Partial rhombencephalosynapsis · Chiari II · DTI · Tractography

L. Merlini (✉) · S. Hanquinet
Unit of Pediatric Radiology, Geneva University Hospital (HUG),
6, Willy-Donzé,
1205 Geneva, Switzerland
e-mail: laura.merlini@hcuge.ch

J. Fluss · C. Korff
Pediatric Neurology, Pediatric Subspecialty Service,
University Hospital of Geneva,
Geneva, Switzerland

Introduction

Chiari type II (CII) malformations refer to a spectrum of congenital hindbrain abnormalities affecting the relationship between the cerebellum, brainstem, upper cervical cord, and the bony skull base. CII involves displacement of brainstem and lower cerebellum into the cervical spinal canal and is nearly always associated with myelomeningocele [1].

Rhombencephalosynapsis (RECS) is a rare posterior fossa malformation characterized by the dorsal fusion of cerebellar hemispheres and agenesis or dysplasia of the vermis [2, 3]. RECS has been described as Gómez–López–Hernández syndrome when it is associated with trigeminal anesthesia and bilateral parietal or parieto-occipital alopecia [4, 5].

Partial rhombencephalosynapsis (PRECS) is described more rarely than RECS and consists of normal anterior vermis and nodulus with deficient posterior vermis and partial fusion of the hemispheres [6]. These observations suggest that RES should be considered as a malformation with variable degrees of severity [7].

The difficulty of discriminating between CII and RECS has been pointed out [8]. In fact, sometimes RECS cases are misinterpreted as having Chiari II malformation, probably because of the rarity of the condition. However, the imaging features of RECS and Chiari II malformations can coexist, and a few cases of CII in combination with RECS have been further reported in the literature [9].

The association of CII with PRECS has also been reported in the literature [10, 11]. However, the true existence of this association is still debated due to the anatomical changes potentially induced by CII [11]. In fact, the small posterior fossa in CII induces a compression of cerebellar hemispheres against one another resulting in the appearance of partly fused hemispheres. CII can thus simply mimic PRECS and the association is doubtful.

Several associated supratentorial abnormalities are sometimes described in RECS: hydrocephalus or ventriculomegaly, dysgenesis, or agenesis of the corpus callosum and absence of the septum pellucidum are the most common [7, 12–14]. However, the presence of these anomalies is not useful to decide if PRECS is present or not in association with CII because the same abnormalities are also described in most cases of isolated CII [9, 15].

In the same manner, there is no typical clinical presentation in RECS that can be useful in discriminating the presence or not of this alteration: It can range from mental retardation to normal intelligence. Seizures are seldom reported in the literature as part of the constellation of symptoms in RECS [11, 13, 16].

The aim of this paper is to illustrate the application of midbrain/hindbrain tractography to a case of CII in which we have found some aspects suggesting PRECS: Our hypothesis was that if findings reported in the literature as typical of RECS could be found in this particular case, we would be allowed to admit that PRECS is associated with CII and not simply "mimicked." This technique has been shown to be relevant in the delineation of various CNS malformations but not in this particular setting.

Case Report

A 13-year-old boy known for spina bifida underwent brain imaging in order to investigate a first episode of complex partial seizure. Previous medical history included neonatal surgery for a lumbar myelomeningocele and the replacement of a long standing ventriculoperitoneal shunt for hydrocephalus 1 year before the present symptoms. Clinically, the patient has no dysmorphic features, in particular no signs suggesting of Gómez–López–Hernández syndrome. Physical exam shows flaccid paraplegia, neurogenic bladder, and mild cerebellar signs on the finger–nose test. In addition, saccadic eyes movements and latent nystagmus are reported. Cognitively, the patient has good social skills, borderline IQ, intermittent dysfluency, low phonological abilities, no signs of callosal disconnection syndrome, normal visuoperceptive skills but difficulties with visuomotor tasks. Academic skills are all severely delayed. Chiari II malformation with midbrain dysgenesis and associated distorted gyral pattern was reported in MR imaging performed 6 years before, but details about the posterior fossa anatomy were lacking.

Imaging Data

MRI study was performed with a 1.5-T magnet using a dedicated 12-channel head coil (Avanto Siemens). Conven-

tional brain MRI showed the classical features of CII malformations consisting of a small posterior fossa, a beaked tectum, and an elongated linear fourth ventricle; the nodulus was very deeply situated and unusually filled by multiple cysts. Moreover, the anterior vermis was present, associated with deficient posterior vermis. The tentorium was thick, interrupted, and horizontal. Aqueductal stenosis was present. Additional supratentorial abnormalities were found consisting of corpus callosum dysgenesis, absent septum pellucidum, interhemispheric cysts, interdigitated gyri with stenogyria, collapsed lateral ventricles, and thin posterior white matter. Superior and middle cerebral peduncles were closely apposed. The continuity of posterior cerebellum hemispheric foliar patterns across the midline was well visible on coronal sequences. The cerebellar hemispheres were "wrapping" around the pons and the medulla and coronal sections demonstrated upward herniation through defected incisura (Fig. 1).

The diffusion tensor imaging (DTI) measurements were performed in addition to a conventional imaging protocol (axial T2-weighted, coronal fluid-attenuated inversion recovery, and 3D SE T1-weighted). The diffusion tensor images were acquired in the axial plane with the following MR parameters: echo time (TE)=92 ms, repetition time= 9,000 ms, integrated parallel acquisition technique=2, Nex 1, field of view 230, matrix 128×128, slice thickness of 2 mm, resulting in a voxel size of 2×2×2 mm, b values=0 and 1,000 s/mm^2, and 30 gradient directions. Diffusion weighting was implemented using a Stejskal–Tanner diffusion scheme (monopolar gradient) in order to achieve shorter TE, better signal/noise ratio, and reduced acquisition time. The DTI sequence duration was 5 min 44 s. Fractional anisotropy (FA) and apparent diffusion coefficient maps and tensor calculation were performed in-line by the MRI scanner.

The FA maps were calculated as the ratio of the anisotropic component of the diffusion tensor to the whole diffusion tensor, as published previously by Basser and Pierpaoli [17]. The 3D orientation of the major eigenvector was color-coded per voxel according to the red–green–blue convention, red indicating a predominant left–right (x-element), green an anterior–posterior (y-element), and blue a superior–inferior (z-element) orientation of the anisotropic component of diffusion within each voxel.

The color intensity scale of the map was scaled in proportion to the measured FA value. The raw data were transferred to an off-line personal computer that was equipped with Osirix open-source software connected automatically to TrackVis software for image registration and fiber tracking. Fiber tracks were calculated using a FACT propagation algorithm from several seed points placed manually at different levels based on the anatomical knowledge of the fiber projection. The samples per voxel

Fig. 1 3D T1 weighted. a
Sagittal: small posterior fossa,
beaked tectum (*arrowheads*),
elongated linear fourth ventricle,
very deeply situated nodulus
with multiple cysts (*long
arrows*) and corpus callosum
dysgenesis (*arrow*). The anterior
vermis is present, associated
with deficient posterior
vermis. The tentorium is thick,
interrupted, and horizontal (*red
arrowheads*). b Axial: inter-
hemispheric cysts, interdigitated
gyri, collapsed lateral ventricles,
thin posterior white matter
and stenogyria (*arrowheads*).
c Coronal: the continuity of
posterior cerebellum hemispheric
foliar patterns across the midline
is well visualized (*arrowheads*)
along with upward herniation of
the cerebellum through defected
incisura. d Coronal: superior and
middle cerebral peduncles are
closely apposed (*arrows*)
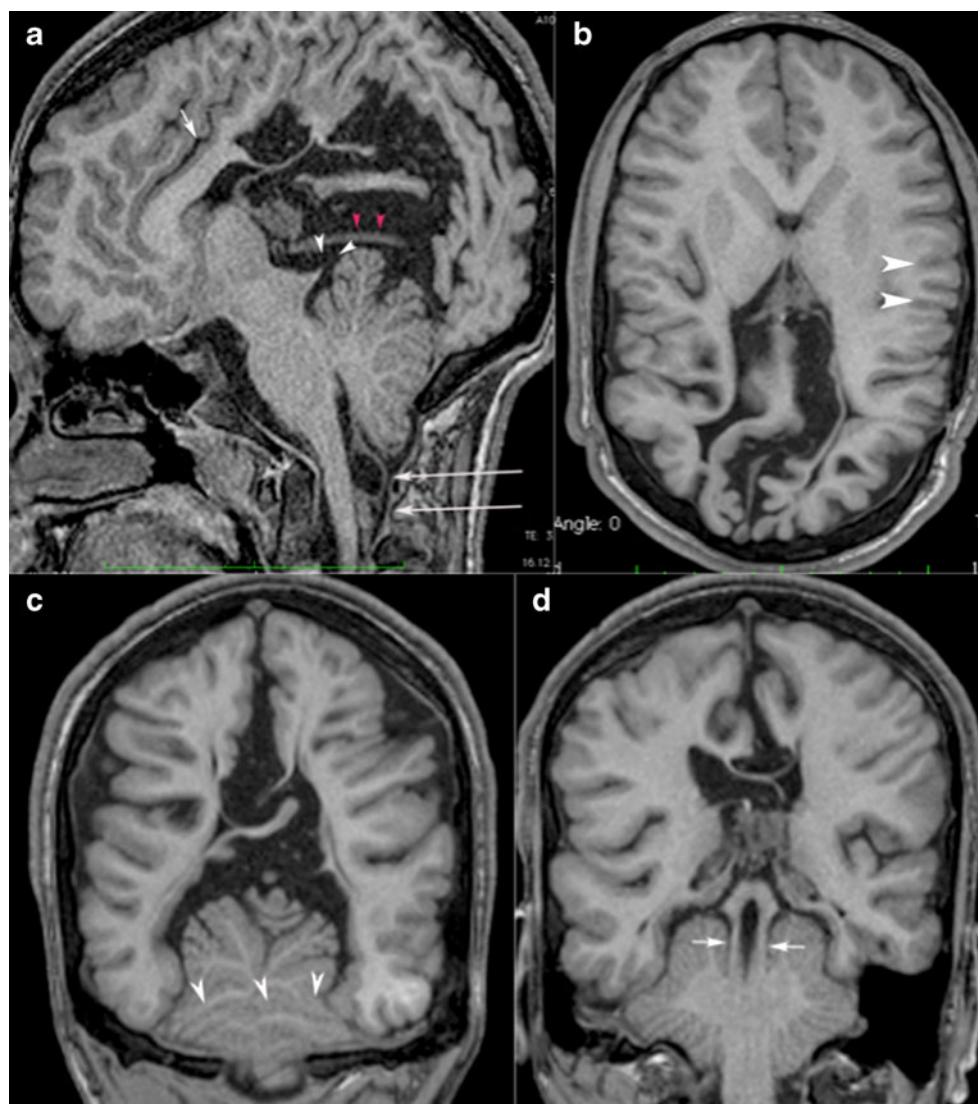
length were 1, with a step length of 1 mm, a curvature
threshold of 0.2, FA threshold of 0.200, and an angle threshold
of 35.00. The same investigator carried out a visual inspection
of the reconstructed trajectories in each subject.

On the color map of DTI at the level of midsection of the
vermis, red-coded transversely oriented fibers are typically seen
in healthy subjects (small arrowheads Fig. 2a). In our patient,
very few red color fibers were visible in this location (small
arrowheads Fig. 2b) due to deficient inferior vermis. In the
medial segments of the fused cerebellum, the fibers were blue-
coded, consistent with a superior–inferior orientation (long
arrows Fig. 2b). These data were confirmed by FT (Fig. 3)

Furthermore, on the DTI color map, a striking lack of
anterior pontine decussation of the middle cerebellar
peduncle (MCP) and a complete absence of the middle
pontine crossing tract were noted (Fig. 2). A very thin
anterior pontine decussation fibers were also visible on the
fiber tracking reconstruction of whole brain on the frontal
view (Fig. 4) in comparison with the normal subject.

Discussion

Our patient presented after a first episode of complex partial
seizure, an occurrence sometimes reported in patients with
RECS [13, 16]: No other clinical signs, such as facial
dysmorphism, trigeminal dysfunction, or alopecia, were
present indicating Gómez–López–Hernández syndrome.
The radiological appearance in our cases of PRECS is
identical to others reported in the literature [10, 11]: The
cerebellar hemispheres have only the inferior part that
seems "fused," and a tiny cleft between them can be
followed in the superior part of the cerebellum in most
cases of PRECS [6]. The nodulus and anterior vermis are
normal, associated with deficient posterior vermis [6, 10].
The supratentorial associated abnormalities are common
both to CII and RECS [3, 8, 13–15].

It is very difficult, if not impossible to assess, whether
the cerebellar hemispheres are fused or only squeezed on
the basis of the conventional MRI. Fiber tracking has rarely

Fig. 2 DTI color map: **a** control; **b** current case. In absence of the inferior vermis (**b**), there are no normal horizontal fibers (**a** *small arrowheads*). Fibers in the medial aspect of the cerebellum run vertically, as demonstrated by the blue color (**b** *long thin arrows*). Moreover, in **b** there is absence of the pontine crossing tract (**a**, **b** *thick arrowheads*)
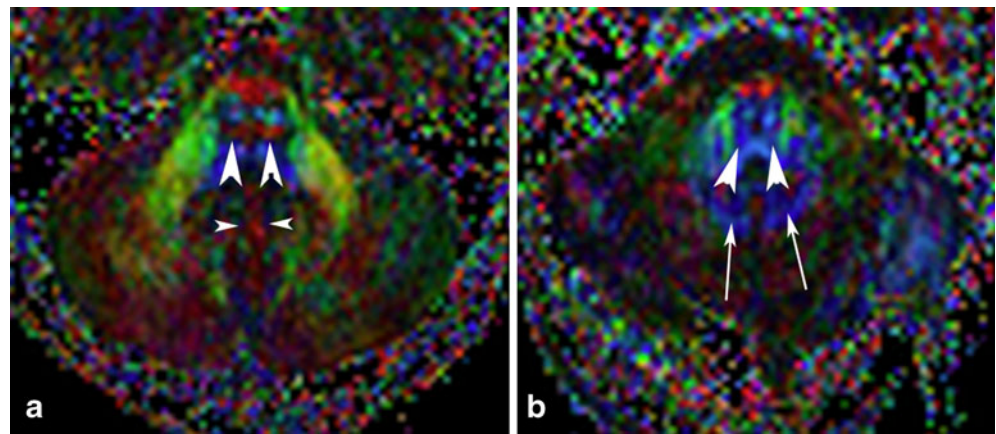
been applied in the study of RECS [18]. In one report, the normal transversely oriented fibers in the midsection of the cerebellar vermis, as demonstrated by red on the color map of DTI, were absent. In the medial segments of the fused cerebellum, the fibers were oriented in a superior–inferior direction. The proximal portions of the superior cerebellar peduncles were also oriented more medially. No abnormalities of the middle cerebellar peduncles and the crossing pontocerebellar fibers were reported.

DTI in CII has rarely been realized [19, 20]. One study focused on posterior fossa abnormalities: The authors used diffusion tensor imaging to search for microstructural alterations of the major cerebellar white matter tracts, the cerebellar peduncles [20].

The FA in the MCP was significantly reduced in the CII patients. The most likely explanation proposed was a reduced fiber density. Moreover, a review on the application of FT in children includes a case of CII with marked hypoplasia of the transverse pontine fibers and underdeveloped superior and inferior cerebellar peduncles [21].

The findings on DTI color map and fiber tracking on the aspect of the cerebellar vermis in our case was in perfect agreement with the observation of Widjaja et al. [18] in a patient with complete RECS. We observed a similar absence of the transverse fibers in the vermis and, on the contrary, a bundle of vertical fibers in the middle part of the cerebellum. It is therefore legitimate to assume that our patient exhibits some anatomical features of RECS. RECS's

Fig. 3 Fiber tracking, posterior view: *a* control; *b* current case. The normal transverse (*red*) vermian fibers are visible in the middle (*a*, *a1*, and *b1 arrowheads*) and scarce in *b*, replaced by aberrant vertical (*blue*) medial fibers (*b1 arrows*). In *b*, the paucity of transverse oriented (*red*) cerebellar hemispheric fibers is also striking
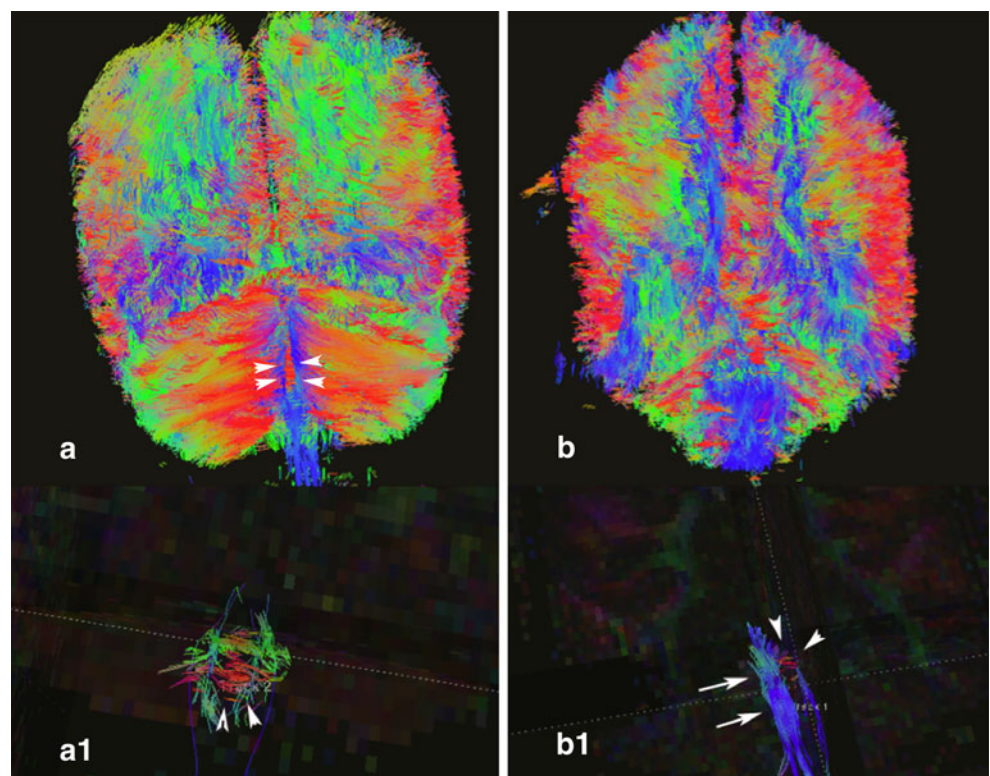
Fig. 4 Fiber tracking, anterior view: *a* control; *b* current case. In *b*, there is a paucity of horizontal fibers corresponding to the anterior pontine decussation (*a, b arrowheads*) compared to the normal subject. In *b1* (*arrows*), the insufficient fibers of middle cerebellar peduncles compared to the normal subject (*a1*) are also well depicted
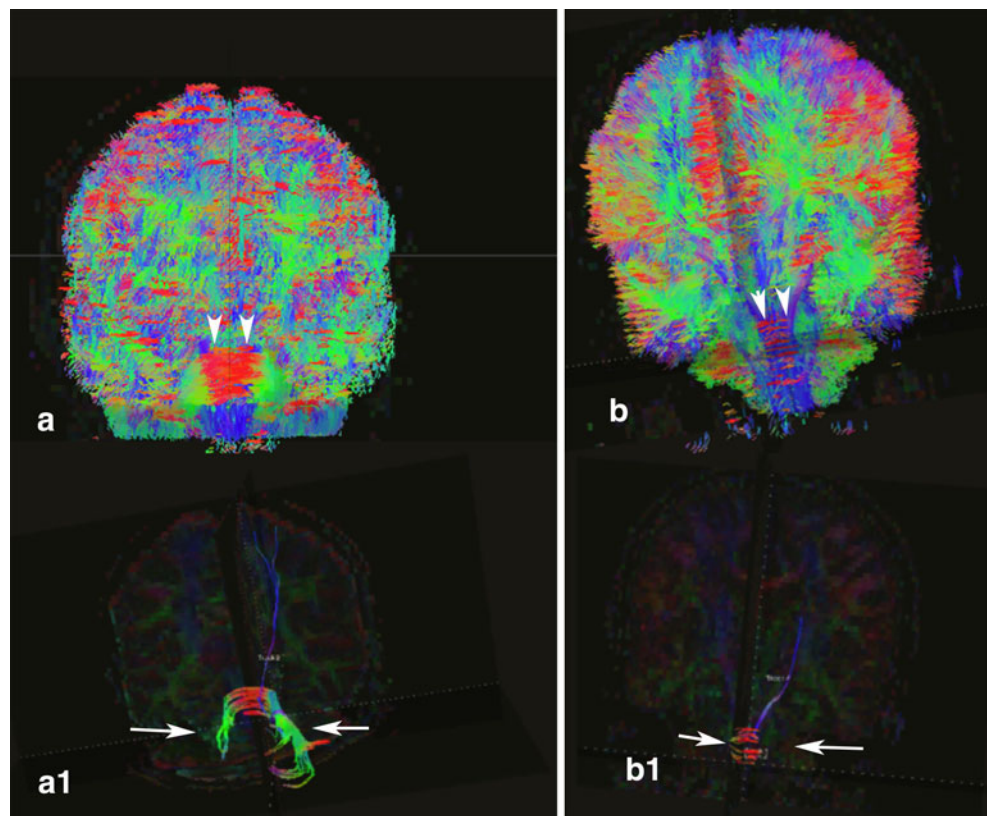
fiber tracking anatomy is peculiar: In other cases of agenesia/hypoplasia of the vermis, such as in Joubert syndrome and related disorders, FT shows the absence of the transverse tract but never the presence of a vertical bundle.

On the other hand, we found an almost complete absence of fibers in the anterior pontine decussation of the MCP compared to normal controls: This observation is in agreement with the findings of Herweh et al. of a reduced number of fibers of the MCP in CII [20]. Moreover, pontine crossing tract fibers are missing in our patient. This is in agreement with the observation of Rollins in one patient with CII malformation [21].

In summary, our study demonstrates overlap of some DTI and tractography aspects of both CII and RECS in a single case. As mentioned before, only few isolated observations are reported in the literature: We could thus assume that this association is casual; however, it can also be postulated that the presence of RECS malformations is not so uncommon in CII but is often unrecognized, due to the small size of the posterior fossa.

A shared embryological pathway cannot, however, be ruled out. The traditional view of embryonic development of the cerebellum arising from two distinct embryonic primordia cannot explain RECS malformation [22, 23]. Sidman and Rakic [24] proposed a different theory, which better explains RECS malformations: This view considers the cerebellar primordium as an unpaired structure that becomes divided into a median vermis and a pair of hemispheres. From that perspective, the fusion of the hemispheres would result from a primary failure of vermian differentiation. The underlying molecular pathway responsible for vermian differentiation is not well understood. It seems that the organization of the cerebellum in sagittal strips or modules is present from an early stage [25]. In this view for example, the paramedian cerebellar cortex, fastigial nucleus, and parts of the ipsilateral olivary nuclei are linked in a single functional sagittal unit.

RECS can be classified among malformations secondary to early rostrocaudal patterning defects of the central stripe due to mutation of a dorsalizing gene such as ZIC2 [26] This mediolateral organization in longitudinal strips of various lengths can explain the presence of various supratentorial midline associations (corpus callosum and septal agenesis) and fusions (thalami and dentate nuclei) along with maldifferentiation of the vermis.

Regarding CII, no single theory fully accounts for all features [27]. Sarnat suggested that abnormal rhombomere formation and ectopic expression of homeobox genes of the rostrocaudal axis of the neural tube might explain CII features [28]. This group of genes may be involved in rhombomeric segmentation as well as programming of the paraxial mesoderm for the basioccipital and supraoccipital bones, resulting in a small posterior fossa if dysfunctional.

Finally, early rostrocaudal patterning defects (i.e., mutation to a dorsalizing gene such as ZIC 2 [28] or Lmx1a [29] could be suggested as a common developmental alteration for both anomalies, RECS and CII, but this remains to be demonstrated. Further studies linking neuroembryology, MRI with DTI and FT, and genetics are a cornerstone to understand the pathway and timing of midbrain/hindbrain malformations.

References

1. Naidich TP, McLone DG, Fulling KH. The Chiari II malformation: part IV. The hindbrain deformity. Neuroradiology. 1983;25(4):179–97.
2. Truwit CL, Barkovich AJ, Shanahan R, Maroldo TV. MR imaging of rhombencephalosynapsis: report of three cases and review of the literature. AJNR Am J Neuroradiol. 1991;12(5):957–65.
3. Jellinger KAK. Rhombencephalosynapsis. Acta Neuropathol. 2002;103(3):305–6.
4. Poretti AA, Bartholdi DD, Gobara SS, Alber FDF, Boltshauser EE. Gomez–Lopez–Hernandez syndrome: an easily missed diagnosis. Eur J Med Genet. 2008;51(3):197–208.
5. Sukhudyan BB, Jaladyan VV, Melikyan GG, Schlump JUJ, Boltshauser EE, Poretti AA. Gómez–López-Hernández syndrome: reappraisal of the diagnostic criteria. Eur J Pediatr. 2010;169(12):1523–8.
6. Demaerel PP, Morel CC, Lagae LL, Wilms GG. Partial rhombencephalosynapsis. AJNR Am J Neuroradiol. 2004;25(1):29–31.
7. Chemli JJ, Abroug MM, Tlili KK, Harbi AA. Rhombencephalosynapsis diagnosed in childhood: clinical and MRI findings. Eur J Paediatr Neurol. 2007;11(1):35–8.
8. Sener RN. Unusual MRI findings in rhombencephalosynapsis. Comput Med Imaging Graph. 2000;24(4):277–82.
9. Sener RN, Dzelzite S. Rhombencephalosynapsis and a Chiari II malformation. J Comput Assist Tomogr. 2003;27(2):257–9.
10. Wan SMSMY, Khong PLSMY, Ip PSMY, Ooi GCSMY. Partial rhombencephalosynapsis and Chiari II malformation. Hong Kong Med J. 2005;11(4):299–302.
11. Ramkumar PGP, Kanodia AKA, Ananthakrishnan GG, Roberts RR. Chiari II malformation mimicking partial rhombencephalosynapsis? A case report. Cerebellum. 2010;9(1):111–4.

12. Toelle SP, Yalcinkaya C, Kocer N, Deonna T, Overweg-Plandsoen WCWCG, Bast TWCG, et al. Rhombencephalosynapsis: clinical findings and neuroimaging in 9 children. Neuropediatrics. 2002;33(4):209–14.
13. Jellinger KAK. Rhombencephalosynapsis with and without associated malformations. Acta Neuropathol. 2009;117(2):219.
14. Boltshauser E. Cerebellum-small brain but large confusion: a review of selected cerebellar malformations and disruptions. Am J Med Genet A. 2004;126A(4):376–85.
15. Miller EE, Widjaja EE, Blaser SS, Dennis MM, Raybaud CC. The old and the new: supratentorial MR findings in Chiari II malformation. Childs Nerv Syst. 2008;24(5):563–75.
16. Striano PP, Morana GG, Pezzella MM, Bellini TT, Rossi AA. Rhombencephalosynapsis in a patient with mental retardation, epilepsy, and dysmorphisms. Neurol Sci. 2011;32(1):193–4.
17. Basser PJ, Pierpaoli C. A simplified method to measure the diffusion tensor from seven MR images. Magn Reson Med. 1998;39(6):928–34.
18. Widjaja E, Blaser S, Raybaud C. Diffusion tensor imaging of midline posterior fossa malformations. Pediatr Radiol. 2006;36(6):510–7.
19. Herweh C, Akbar M, Wengenroth M, Blatow M, Mair-Walther J, Rehbein N, et al. DTI of commissural fibers in patients with Chiari II-malformation. Neuroimage. 2009;44(2):306–11.
20. Herweh CC, Akbar MM, Wengenroth MM, Heiland SS, Bendszus MM, Stippich CC. Reduced anisotropy in the middle cerebellar peduncle in Chiari-II malformation. Cerebellum. 2010;9(3):303–9.
21. Rollins NKN. Clinical applications of diffusion tensor imaging and tractography in children. Pediatr Radiol. 2007;37(8):769–80.
22. Barth PGP. Rhombencephalosynapsis. Handb Clin Neurol. 2008;87:53–65.
23. Utsunomiya H, Takano K, Ogasawara T, Hashimoto T, Fukushima T, Okazaki M. Rhombencephalosynapsis: cerebellar embryogenesis. AJNR Am J Neuroradiol. 1998;19(3):547–9.
24. Sidman RL, Rakic P. Development of the human central nervous system. In: Haymaker W, Adams RD, editors. Histology and histopathology of the nervous system. Springfield: Thomas; 1982. p. 3–145.
25. Herrup K, Kuemerle B. The compartmentalization of the cerebellum. Annu Rev Neurosci. 1997;20:61–90.
26. Barkovich AJ, Millen KJK, Dobyns WBW. A developmental and genetic classification for midbrain–hindbrain malformations. Brain. 2009;132(Pt 12):3199–230.
27. Tubbs RS, Shoja MM, Ardalan MRM, et al. Hindbrain herniation: a review of embryological theories. Ital J Anat Embryol. 2008;113:37–46.
28. Sarnat HB. Molecular genetic classification of central nervous system malformations. J Child Neurol. 2000;15(10):675–87.
29. Chizhikov VV, Lindgren AG, Mishima Y, Roberts RW, Aldinger KA, Miesegaes GR, Currle DS, Monuki ES, Millen KJ. Lmx1a regulates fates and location of cells originating from the cerebellar rhombic lip and telencephalic cortical hem. Proc Natl Acad Sci USA. 2010;107(23):10725–30.